Increasing Throughput in Fused Deposition Modeling by Modulating Bed Temperature

Kelsey L. Snapp
Department of Mechanical Engineering,
Boston University,
110 Cummington Mall,
Boston, MA 02215
e-mail: ksnapp@bu.edu

Aldair E. Gongora
Department of Mechanical Engineering,
Boston University,
110 Cummington Mall,
Boston, MA 02215
e-mail: agongora@bu.edu

Keith A. Brown[1]
Mem. ASME
Department of Mechanical Engineering,
Boston University,
110 Cummington Mall,
Boston, MA 02215
e-mail: brownka@bu.edu

Additive manufacturing (AM) techniques, such as fused deposition modeling (FDM), are able to fabricate physical components from three-dimensional (3D) digital models through the sequential deposition of material onto a print bed in a layer-by-layer fashion. In FDM and many other AM techniques, it is critical that the part adheres to the bed during printing. After printing, however, excessive bed adhesion can lead to part damage or prevent automated part removal. In this work, we validate a novel testing method that quickly and cheaply evaluates bed adhesion without constraints on part geometry. Using this method, we study the effect of bed temperature on the peak removal force for polylactic acid (PLA) parts printed on bare borosilicate glass and polyimide (PI)-coated beds. In addition to validating conventional wisdom that bed adhesion is maximized between 60 and 70 °C (140 and 158 °F), we observe that cooling the bed below 40 °C (104 °F), as is commonly done to facilitate part removal, has minimal additional benefit. Counterintuitively, we find that heating the bed after printing is often a more efficient process for facile part removal. In addition to introducing a general method for measuring and optimizing bed adhesion via bed temperature modulation, these results can be used to accelerate the production and testing of AM components in printer farms and autonomous research systems. [DOI: 10.1115/1.4050177]

Keywords: fused deposition modeling (FDM), bed adhesion, removal temperature, additive manufacturing, process engineering, sensing, monitoring and diagnostics

1 Introduction

Additive manufacturing (AM), the process of building an object layer-by-layer from a three-dimensional (3D) digital model, has experienced tremendous growth for rapid prototyping and producing parts in small volume or with complex geometries [1]. Among the myriad and growing families of AM [2], material extrusion (ME), commonly known as fused deposition modeling (FDM) or fused filament fabrication (FFF), is a popular method for AM because of its low cost and ease of use. In FDM, thermoplastic polymer filament is pushed through a heated nozzle and deposited onto a print bed [3,4]. Despite the simplicity of this approach, selecting process parameters for successful printing can often be subtle, which has sparked numerous studies focusing on process parameters such as extruder temperature, layer thickness, raster width, raster orientation, air gap, bed temperature, print speed, and print orientation [5–11]. An additional and less studied property is bed adhesion, which refers to the adhesion between the part and the printer bed. Bed adhesion is a critical factor to manage since insufficient adhesion can lead to premature detachment of the part from the bed, resulting in a failed print [12–14].

With a focus on avoiding failed prints from low adhesion, several studies have sought to maximize adhesion by modulating bed temperature and bed composition [15–17]. While achieving high adhesion is desirable during printing, high adhesion is undesirable after printing has concluded because the part could be damaged during removal. Further, automated part retrieval has been demonstrated as a method for dramatically accelerating part production and mechanical design, but it requires careful tuning of adhesion to enable robotic retrieval [18,19]. To circumvent the need for automated part removal from the bed, one can automatically replace the entire build plate after each print; however, this approach prevents automated mechanical testing [20]. To minimize adhesion after printing, common practice is to let the bed cool to room temperature [13], but this practice has not been systematically evaluated. In order to accelerate automated part retrieval in AM, a basic understanding of how to efficiently manage adhesion during and after printing is needed.

Here, we study the peak force required to remove a part printed using FDM as a function of bed temperature on both bare and polyimide (PI)-coated glass beds. Initially, we identify a simple and transferable approach to rapidly measure the peak removal force required to remove a part from the printer bed, which can be used to study different part geometries. In order to independently evaluate the effect of adhesion during and after the print, we conduct studies with distinct temperatures during and after printing. Through a systematic study of removal force versus bed temperature, we determine the optimal print bed temperature, the minimum effective removal temperature, and several benefits of heating rather than cooling for part removal. Finally, we evaluate the complete cycle time associated with printing and removing parts and find that, strikingly, heating after printing is more efficient than cooling after printing. In addition to being of fundamental interest to the AM community, this bears important implications for FDM-based autonomous research and high throughput AM. While the discussion here is limited to polylactic acid (PLA) cylinders, the simplicity of this testing approach would allow researchers to rapidly evaluate other chemistries or geometries. Given the dramatic increase in interest in custom filaments for FDM, we anticipate that optimizing adhesion for emerging materials will only increase in importance [21–23].

2 Material and Methods

2.1 Design and Fabrication. Unless otherwise specified, the hollow cylindrical parts used in this study were designed using OPENSCAD to be 20 mm (0.79 in.) in radius and 30 mm (1.2 in.) in height. The G-code for the parts was generated using SLIC3R and then sent to the FDM 3D printer (Makergear M2) using REPETIER. The parts were printed using PLA (Makergear) filament and a 0.35 mm (0.014 in.) diameter brass extrusion nozzle. The parts were either printed directly on a borosilicate glass bed (Makergear) or a borosilicate glass bed coated with a 51 mm (2 in.) wide strip of

[1]Corresponding author.
Manuscript received June 15, 2020; final manuscript received February 1, 2021; published online April 1, 2021. Assoc. Editor: Sam Anand.

PI tape (Makergear). The PI film was replaced if damage such as tears or bubbles was observed. Although it is common for PI films to be used for many months before replacement, the high removal forces in some of our experiments caused premature damage. Therefore, we inspected the film following each set of experiments to ensure that all samples were printed under identical conditions.

The hollow cylindrical parts were printed with three top layers, three bottom layers, two perimeter lines, a 0.39 mm (0.015 in.) perimeter line width, no infill, and an alternating rectilinear pattern for the top and bottom layers. The layer height was set to 0.3 mm (0.012 in.), with the exception of the first layer height, which was set to 0.35 mm (0.014 in.). No initial layer height adjustments were made to compensate for the thickness of the PI film. The first layer was printed at 30 mm/s (1.2 in./s) while subsequent layers were printed at 60 mm/s (2.4 in./s), with the exception of the outermost perimeter, which was printed at 30 mm/s (1.2 in./s) for all layers. Bed temperature was measured using the Makergear M2's temperature interface. When a print was started, the bed and nozzle were heated to the required temperatures. The nozzle was set to 220 °C (428 °F) for all prints. The bed print temperature T_p was set to either 60 or 70 °C (140 or 158 °F). This range was chosen as, during our initial tests, bed print temperatures above or below these values commonly resulted in failed prints on the glass bed. The print would start when both the bed and nozzle temperatures reached their set points, as measured by the M2's built-in temperature interface. The extruder fan was set to 0% for the first three layers, and then to 100% for subsequent layers. After the print ended, the bed temperature was set to the removal temperature T_r. Part removal started immediately upon reaching the target bed temperature, and removal of all specimens on the bed typically took less than a minute. For each production cycle, three cylinders were printed on glass and three were printed on PI-coated glass. Therefore, six cylinders were printed simultaneously. For each set of conditions tested, three production cycles were conducted, providing nine data points for each unique parameter combination.

2.2 Testing Procedure. During testing, the peak removal force was measured using a digital force gauge (HF-500), which has a 0.1 N (0.02 lbf) resolution and a 5 N (1.1 lbf) minimum detectable force. The gauge was placed horizontally with the tip centered on the top of the cylinder. Increasing pressure was applied laterally until the part completely released from the bed surface or until the part broke. The peak measured force was recorded as the removal force F_r. If the $F_r < 5$ N (1.1 lbf), then 0 N (0 lbf) was taken as F_r as the sensor could not register forces below its threshold value. If the part broke before removal, the peak force prior to the break was taken as F_r. Each temperature condition was evaluated for nine identically prepared samples for a total of approximately 400 tested cylinders.

3 Results and Discussion

In order to rapidly evaluate part-bed adhesion in FDM, we sought to develop a facile method to measure the force required to remove a part from the bed after printing. Prior methods either relied upon shearing thin strips of printed material that were three layers tall [17] or involved pulling parts vertically away from the print bed [15,16]. While these methods provide valuable insight, they require the development of an expensive testing system and do not directly measure the forces required to remove parts in practice. Thus, we hypothesized that pushing a part laterally with a force gauge while recording the peak force would more closely resemble how humans or robots remove parts from the print bed in practice. Pushing laterally on a part with a force gauge is likely not the most efficient method of part removal in terms of minimizing the force required. For example, a two-sided gripper could impart a controlled torque along with a lateral force and also have superior control over the part after removal. However, the force gauge method used here provides repeatability at low cost, allowing operators to quickly evaluate the ideal print conditions for their part. For this reason, we believe it could be a useful tool for studying adhesion and optimizing print parameters.

We developed a facile process for measuring the adhesion between FDM printed components and the bed (see Table 1 and Sec. 2). In brief hollow cylindrical parts were printed on either bare glass or PI-coated glass at a constant bed temperature T_p and constant nozzle temperature T_{noz} (Figs. 1(*a*) and 1(*b*)). Subsequently, the bed was heated or cooled to the removal bed temperature T_r and then the force gauge was used to remove the part through an application of force that was subsequently recorded (Fig. 1(*c*)) with the maximum force being recorded as F_r (Fig. 1(*d*)). While this force was representative of what is required to remove a specific part, whether this force provides any predictive information that is transferrable to other part geometries was not known.

To test whether the force needed to remove a part can be interpreted in a general context, we performed a series of adhesion tests on 90 cylinders with varying geometries. For instance, as the cylinder radius was increased from 16 to 24 mm (0.63 to 0.94 in.), F_r for parts printed on PI was found to increase by 50% (Fig. 2(*a*)). Interestingly, F_r required for parts printed on glass exhibited a similar increase, albeit with a lower magnitude. Qualitatively, the need for a larger force is consistent with the larger contact area between the part and the build plate, resulting in stronger adhesion. In contrast, as the cylinder height was increased, F_r was observed to decrease (Fig. 2(*b*)), which we hypothesize was due to a longer moment arm between the applied force and the part-bed interface. While these measurements have large standard deviations, one-way analysis of variance shows that these points have a less than 0.1% chance of reflecting the same distributions. Similarly, the trend for parts printed on bare glass was consistent with that exhibited on PI-coated glass albeit with a lower magnitude. From these results, we conclude that while the absolute F_r depended on the part geometry, the ratio of F_r between glass and PI remained statistically indistinguishable (p-values significantly above 0.05) in all geometry-based experiments (Fig. 2(*c*)). Specifically, for all 90 specimens, the average ratio was 0.27 with a standard deviation of 0.10, which implies that, at this removal temperature, parts printed on PI required ~3.5 times more force to remove than parts printed on glass. This shows that, at least in a relative sense, this testing method allows one to measure a quantity that is reflective of the fundamental interaction between the part and the bed. Further, this implies that upon using a standard part geometry, measuring F_r can allow one to study how altering processing parameters affects adhesion.

Having shown that F_r for a specific part is of fundamental value, we sought to determine whether other factors could result in robust control over adhesion. Specifically, it is important to maximize adhesion during printing to prevent print failure, but after printing, low adhesion is preferable to facilitate part removal. Thus, we hypothesized—building off conventional wisdom of the FDM community—that modulating bed temperature could be a rapid path to dynamically tuning adhesion. To explore this, 288 hollow cylinders (see Table 2 and Sec. 2) were printed using various T_p and T_r (Fig. 3). Two major trends were immediately apparent: (1) PI robustly exhibited larger F_r and (2) F_r was maximized when

Table 1 Cylinders of various heights *h* and radii *r* were printed on both glass and PI substrates

	Height *h*		
Radius *r*	15 mm (0.59 in.)	30 mm (1.2 in.)	45 mm (1.8 in.)
16 mm (0.63 in.)	0	9 PI, 9 glass	0
20 mm (0.79 in.)	9 PI, 9 glass	9 PI, 9 glass	9 PI, 9 glass
24 mm (0.94 in.)	0	9 PI, 9 glass	0

Note: In all, 90 samples were printed to test different geometries.

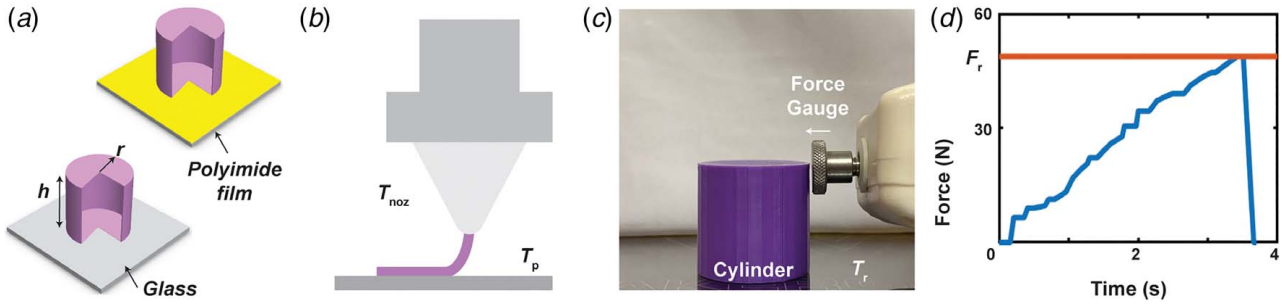

Fig. 1 (*a*) Hollow cylinders are printed on bare glass or polyimide (PI)-coated glass. (*b*) During printing, filament is extruded through a nozzle held at 220 °C onto a bed with temperature T_p at either 60 or 70 °C. (*c*) After the print was finished, the bed was heated or allowed to cool to the removal temperature T_r. A force gauge was placed horizontally with the tip centered on the top edge of the part. The lateral force was manually increased until the part broke free from the bed. (*d*) The maximum force recorded by the force gauge was taken as the removal force F_r.

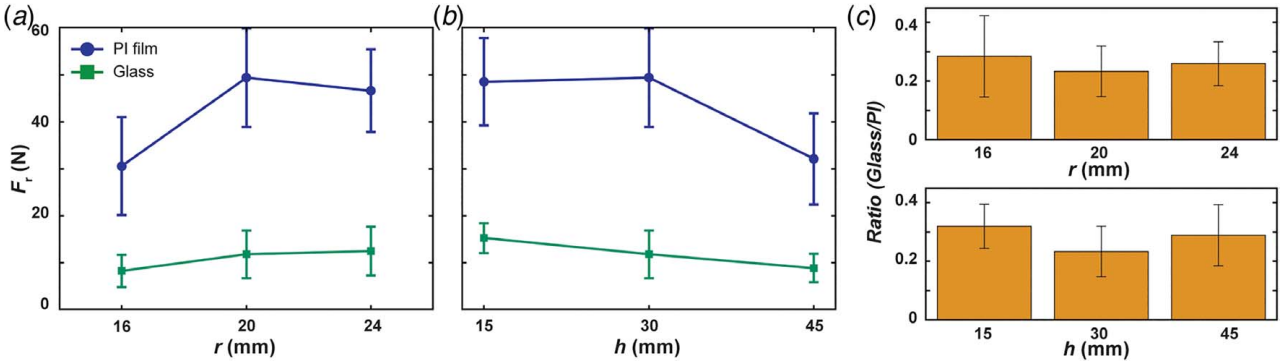

Fig. 2 (*a*) Measured F_r for hollow cylinders of varying radius r but a fixed height $h = 30$ mm, (*b*) measured F_r for hollow cylinders of varying h but fixed $r = 20$ mm, and (*c*) ratio of F_r measured on glass to that measured on PI. In all panels, error bars denote standard deviation, $T_p = 60$ °C, and $T_r = 80$ °C.

T_r ~60–70 °C (140–158 °F) with lower adhesion observed at hotter or colder temperatures. Intriguingly, F_r always appeared to be maximized when T_p differed from T_r. Specifically, when printing at 60 °C (140 °F), the force was largest when removing the part at 70 °C (158 °F) and vice versa. While these points exhibited a great deal of variation and these trends could be due to limited statistics, it is interesting to hypothesize mechanisms that might lead to such a trend. For instance, perhaps printing at 70 °C (158 °F) results in more conformal contact between the part and bed, but the work of adhesion is higher at 60 °C (140 °F). This phenomenon warrants further study.

Interestingly, significantly greater variance of F_r was found at $T_r = 60$ °C (140 °F). We believe that this is because the glass transition temperature of PLA is ~60 °C (140 °F) [17], leading to slight variations in bed temperature having an outsized effect on adhesion. This hypothesis could be tested by performing equivalent studies with materials that have a higher or lower glass transition temperature.

Table 2 Identical cylinders ($r = 20$ mm (0.79 in.), $h = 30$ mm (1.2 in.)) were printed on both PI and glass beds

	Print temperature T_p	
Removal temperature T_r	60 °C (140 °F)	70 °C (158 °F)
30 °C (86 °F)	9 PI, 9 glass	9 PI, 9 glass
40 °C (104 °F)	9 PI, 9 glass	9 PI, 9 glass
50 °C (122 °F)	9 PI, 9 glass	9 PI, 9 glass
60 °C (140 °F)	9 PI, 9 glass	9 PI, 9 glass
70 °C (158 °F)	9 PI, 9 glass	9 PI, 9 glass
80 °C (176 °F)	9 PI, 9 glass	9 PI, 9 glass
90 °C (194 °F)	9 PI, 9 glass	9 PI, 9 glass
100 °C (212 °F)	9 PI, 9 glass	9 PI, 9 glass

Note: Bed temperature T_p during printing was set at either 60 °C (140 °F) or 70 °C (158 °F). Bed temperature T_r during removal ranged from 30 to 100 °C (86 to 212 °F) in increments for 10 °C (18 °F).

The systematic study of T_r provided several important observations with relevance to efficient FDM. (1) In a validation of common practice, cooling the bed after printing made parts significantly easier to release. Interestingly, 40 °C (104 °F) was the most effective choice for T_r as $T_r < 40$ °C (104 °F) showed no additional reduction in F_r. (2) The consistently higher F_r observed when printing on PI was promising for avoiding adhesion-related print failures, but its substantially higher floor posed a barrier to facile automated, or manual, part retrieval. Thus, counterintuitively, glass beds may likely be superior for high throughput manufacturing. (3) Strikingly, for PI, heating after printing may be more effective than cooling at lowering F_r. In particular, F_r only decreased ~50% when testing on PI-coated glass when $T_r < T_p$. However, for $T_r > T_p$, decreases in F_r of 80–90% were observed. An additional tradeoff observed for heating after printing, however, was that heating the bed to 90–100 °C (194–212 °F) sometimes led to warping or deformation of the bottom of the part, highlighting the need for part-specific testing.

While we did not observe any drawbacks to having high adhesion during printing, care is warranted when minimizing adhesion after printing by elevating temperature as we observed several instances of plastic deformation during removal at temperatures ≥90 °C (194 °F), especially when printing on PI film. Interestingly, while parts printed on PI film sometimes failed during removal, they did so in one of two distinct regimes. When $T_r = 60$ or 70 °C (140 or 158 °F), parts sometimes failed by interlayer delamination as the removal force overcame interlayer bonding. However, at

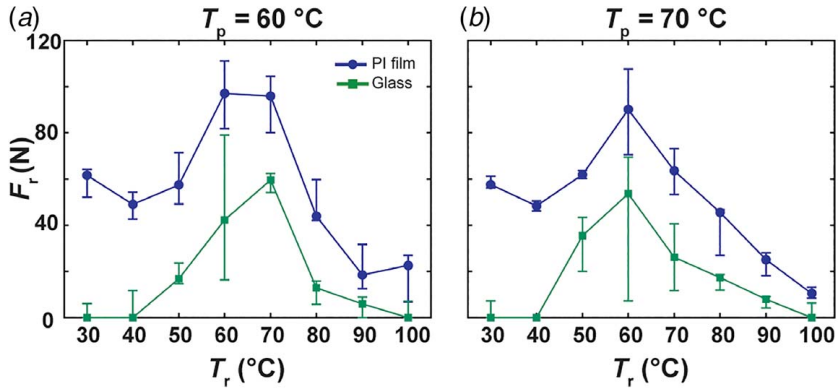

Fig. 3 Measured F_r for various T_r with (*a*) $T_p = 60$ °C and (*b*) $T_p = 70$ °C. Error bars denote the 25th and 75th quartiles.

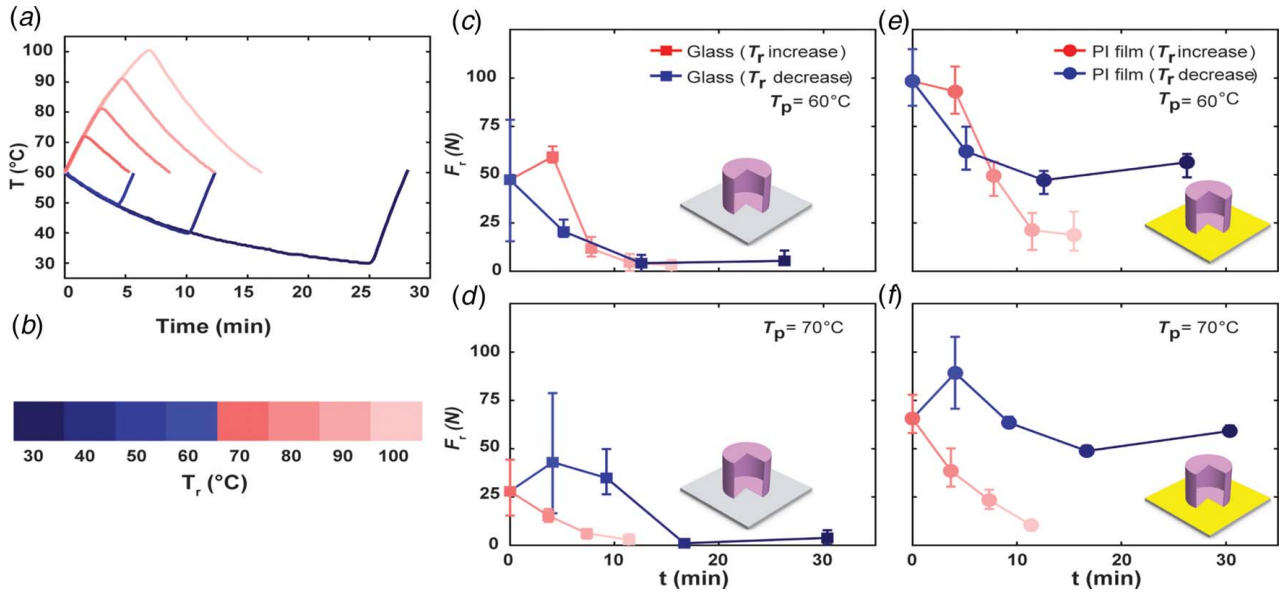

Fig. 4 (*a*) Experimental temperature *T* versus time profiles that depict cycling the system from $T_p = 60$ °C to various T_r and back to T_p when room temperature was 20 °C. The time to return was denoted the cycle time *t*. For a given target T_r shown as the (*b*) scale, F_r can be related to *t* for (c) $T_p = 60$ °C on a bare glass bed, (*d*) $T_p = 70$ °C on a bare glass bed, (e) $T_p = 60$ °C on a PI-coated glass bed, and (*f*) $T_p = 70$ °C on a PI-coated glass bed.

$T_r \geq 90$ °C (194 °F), the heated parts sometimes buckled due to lower structural integrity cause by the higher bed temperature softening the part. Interlayer delamination was also occasionally seen at these higher temperatures, although less often. Importantly, no parts that were printed on glass were damaged during removal. Thus, we do not believe that there is a single ideal removal process for all situations, but rather that heating should be considered as an alternative to cooling to accelerate the process. Importantly, the rapid method for measuring adhesion is an important part of evaluating potential strategies for accelerating part removal.

The observation that heating after printing may be superior to cooling raises the further question of whether this could be faster from the perspective of printing cycle time. Thus, defining the cycle time t to be the time required to heat/cool the bed from T_p to T_r and back, it is clear from the measured trajectories of the bed temperature that heating was faster than cooling for a given temperature swing (Fig. 4(*a*)). This is because the cooling rate is faster at temperatures further from room temperature. Additionally, the heating rate was faster than the cooling rate as the speed of heating was determined by the strength of the heater while cooling required convective/conductive transport into the surrounding environment. Considering two cycles with equivalent total temperature swings, cycling the bed between 60 °C (140 °F) and 90 °C (194 °F) took $t = 12.3$ min, while cycling the bed between 60 °C (140 °F) and 30 °C (86 °F) took $t = 28.2$ min. When these trajectories were combined with measurements of F_r, they allowed us to compute F_r versus t (Figs. 4(*c*)–4(*f*)). Critically, these plots depict the tradeoffs inherent to minimizing both F_r and t. For instance, when $T_p = 70$ °C (158 °F) on either bare glass or PI-coated glass (Figs. 4(*d*) and 4(*f*)), heating to 80 °C (176 °F) provided a more than 50% decrease in F_r while taking less than 5 min. Out of all the conditions tested, cooling was only consistently more efficient when $T_p = 60$ °C (140 °F) on bare glass (Fig. 4(*c*)). This process would also allow one to evaluate the acceleration afforded by hardware alterations such as the addition of a fan or stronger heater to reduce cycle time.

4 Conclusion

Ultimately, this work represents a roadmap for implementing a testing protocol to quickly determine the optimum conditions for a specific printer both in terms of maximizing adhesion during

printing and minimizing cycle time between prints. With the expanding influence of FDM and advent of 3D printing farms and autonomous research systems based on AM, managing part adhesion to efficiently swing between high adhesion during printing and low adhesion during removal is of critical importance. Here, we explored both T_r and bed material to elucidate optimal conditions for managing these disparate constraints. Key takeaways include:

- A novel and easy-to-implement testing method was developed that replicates how humans and robots remove parts to quickly and cheaply measure F_r. This testing method was validated by testing F_r for parts of varying geometry to find that PI-coating a glass bed increases F_r by ~3.5 fold across various print bed temperatures and cylinder shapes.
- By exploring F_r versus T_r, we found that not only can heating be more effective at decreasing F_r, but that it may also lead to quicker cycle times. Printing a single object at a time brings significant advantages on an FDM printer, such as eliminating travel time between parts and improving part surface finish. However, job times for single-part prints are significantly shorter, making it critical to minimize the downtime between prints. Thus, these results will have high relevance to both small-batch manufacturing and autonomous research using AM.
- Finally, $T_r < 40$ °C (104 °F) did not further decrease F_r, showing a point of diminishing return in the conventional method of allowing the bed to cool after printing.

Acknowledgment

This work was supported by Google LLC, the Boston University Rafik B. Hariri Institute for Computing and Computational Science & Engineering, the National Science Foundation (CMMI-1661412), and the US Army CCDC Soldier Center (contract W911QY2020002).

Conflict of Interest

There are no conflicts of interest.

Data Availability Statement

The datasets generated and supporting the findings of this article are obtainable from the corresponding author upon reasonable request. The authors attest that all data for this study are included in the paper. Data provided by a third party are listed in Acknowledgment.

Nomenclature

h = height of test cylinder
r = radius of test cylinder
F_r = peak force required to dislodge part from bed
T_{noz} = temperature of nozzle when printing
T_p = temperature of bed when printing part
T_r = temperature of bed when removing part

References

[1] Huang, Y., Leu, M. C., Mazumder, J., and Donmez, A., 2015, "Additive Manufacturing: Current State, Future Potential, Gaps and Needs, and Recommendations," ASME J. Manuf. Sci. Eng. Trans., **137**(1), pp. 1–10.
[2] ASTM International, 2013, "F2792-12a—Standard Terminology for Additive Manufacturing Technologies," Rapid Manuf. Assoc.
[3] Bellini, A., Güçeri, S., and Bertoldi, M., 2004, "Liquefier Dynamics in Fused Deposition," ASME J. Manuf. Sci. Eng. Trans., **126**(2), pp. 237–246.
[4] Beaman, J. J., Bourell, D. L., Seepersad, C. C., and Kovar, D., 2020, "Additive Manufacturing Review: Early Past to Current Practice," ASME J. Manuf. Sci. Eng., **142**(11), pp. 1–20.
[5] Krotký, J., Honzíková, J., and Moc, P., 2016, "Deformation of Print PLA Material Depending on the Temperature of Reheating Printing Pad," Manuf. Technol., **16**(1), pp. 136–140.
[6] Khatwani, J., and Srivastava, V., 2018, "Effect of Process Parameters on Mechanical Properties of Solidified PLA Parts Fabricated by 3D Printing Process," 3D Print. Addit. Manuf. Technol., pp. 95–104.
[7] Arbeiter, F., Spoerk, M., Wiener, J., Gosch, A., and Pinter, G., 2018, "Fracture Mechanical Characterization and Lifetime Estimation of Near-Homogeneous Components Produced by Fused Filament Fabrication," Polym. Test., **66**, pp. 105–113.
[8] Abbott, A. C., Tandon, G. P., Bradford, R. L., Koerner, H., and Baur, J. W., 2018, "Process-Structure-Property Effects on ABS Bond Strength in Fused Filament Fabrication," Addit. Manuf., **19**, pp. 29–38.
[9] Ang, K. C., Leong, K. F., Chua, C. K., and Chandrasekaran, M., 2006, "Investigation of the Mechanical Properties and Porosity Relationships in Fused Deposition Modelling-Fabricated Porous Structures," Rapid Prototyp. J., **12**(2), pp. 100–105.
[10] Ahn, S. H., Montero, M., Odell, D., Roundy, S., and Wright, P. K., 2002, "Anisotropic Material Properties of Fused Deposition Modeling ABS," Rapid Prototyp. J., **8**(4), pp. 248–257.
[11] Thrimurthulu, K., Pandey, P. M., and Reddy, N. V., 2004, "Optimum Part Deposition Orientation in Fused Deposition Modeling," Int. J. Mach. Tools Manuf., **44**(6), pp. 585–594.
[12] Devicharan, R., and Garg, R., 2018, "Optimization of the Print Quality by Controlling the Process Parameters on 3D Printing Machine," 3D Print. Addit. Manuf. Technol., pp. 187–194.
[13] Singh, K., 2018, "Experimental Study to Prevent the Warping of 3D Models in Fused Deposition Modeling," Int. J. Plast. Technol., **22**(1), pp. 177–184.
[14] Spoerk, M., Gonzalez-Gutierrez, J., Lichal, C., Cajner, H., Berger, G. R., Schuschnigg, S., Cardon, L., and Holzer, C., 2018, "Optimisation of the Adhesion of Polypropylene-Based Materials During Extrusion-Based Additive Manufacturing," Polymers, **10**(5), p. 490.
[15] Płaczek, D., 2019, "Adhesion Between the Bed and Component Manufactured in FDM Technology Using Selected Types of Intermediary Materials," MATEC Web Conf., **290**, p. 01012.
[16] Teliskova, M., Torek, J., Cmorej, T., Kocisko, M., and Petrus, J., 2017, "Adjustments of RepRap Type Printer Workbench," 2017 4th International Conference on Industrial Engineering and Applications, Nagoya, Japan, Apr. 21–23, ICIEA, pp. 15–19.
[17] Spoerk, M., Gonzalez-Gutierrez, J., Sapkota, J., Schuschnigg, S., and Holzer, C., 2018, "Effect of the Printing Bed Temperature on the Adhesion of Parts Produced by Fused Filament Fabrication," Plast. Rubber Compos., **47**(1), pp. 17–24.
[18] Gongora, A. E., Xu, B., Perry, W., Okoye, C., Riley, P., Reyes, K. G., Morgan, E. F., and Brown, K. A., 2020, "A Bayesian Experimental Autonomous Researcher for Mechanical Design," Sci. Adv., **6**(15), p. eaaz1708.
[19] Gongora, A. E., Snapp, K. L., Whiting, E., Riley, P., Reyes, K. G., Morgan, E. F., and Brown, K. A., 2021, "Using Simulation to Accelerate Autonomous Experimentation (AE): A Case Study Using Mechanics," SSRN Electron. J.
[20] "Collaborative Robots Help Triples 3D Printing Production at Voodoo Manufacturing." https://www.universal-robots.com/case-stories/voodoo-manufacturing/, Accessed March 4, 2020.
[21] Aravind, A. U., Bhagat, A. R., and Radhakrishnan, R., 2020, "A Novel Use of Twisted Continuous Carbon Fibers in Additive Manufacturing of Composites," Mater. Today Proc.
[22] Marasso, S. L., Cocuzza, M., Bertana, V., Perrucci, F., Tommasi, A., Ferrero, S., Scaltrito, L., and Pirri, C. F., 2018, "PLA Conductive Filament for 3D Printed Smart Sensing Applications," Rapid Prototyp. J., **24**(4), pp. 739–743.
[23] Lee, D., Lee, Y., Lee, K., Ko, Y., and Kim, N., 2019, "Development and Evaluation of a Distributed Recycling System for Making Filaments Reused in Three-Dimensional Printers," ASME J. Manuf. Sci. Eng. Trans., **141**(2), p. 021007.